Chapter 2

Dynamic Modeling of Flexible Link Manipulator

2.1 Introduction

The first step in control design process is to develop an appropriate mathematical model of a physical system. Advanced control mechanisms like SMC, feedback linearization, $H\infty$ are model based controls. The requirement of robust, accurate control necessitates advanced control design, which in turn demands accurate mathematical model. Although no model can perfectly represent a dynamical system, model should be able to capture adequate system dynamics. Challenges faced for developing a mathematical model of a flexible link manipulator (FLM) have been discussed in the previous chapter.

In this Chapter, a dynamic model of a single link flexible manipulator (SFLM) is derived first. This model is used for the development of different sliding mode controllers in the subsequent chapters. The dynamic equations of SLFM are derived using the Euler Lagrangian approach. The flexible link is assumed as a rotatory spring rotating about its axis. It is modeled using lumped parametric method where in the flexibility is captured by discrete, localized masses and springs. The equations of motion of the SLFM are derived in terms of the independent generalized coordinates.

FLMs are widely used in space robotics, which are rarely found in single link form. To enhance the maneuver capability, single link is inadequate and hence multi link manipulators are used in many of the applications. Control challenges increase as the plant changes from single link to multiple links. Therefore it is important to develop controllers for multi link flexible manipulator. As a representative case of this category, a two link flexible manipulator (TLFM) is taken as a plant under study.

Initially mathematical model of TLFM is derived with a simple decoupled approach. In this approach, both the links along with their hubs are treated as two independent single flexible links and both the drives are controlled independently. Mathematical model of the individual link is developed using lumped parametric approach. This generates a simple but approximate model of the TLFM system.

Further to improve modeling accuracy, distributed modeling approach is used. Here a TLFM is treated as a continuous dynamic system, where the dynamics of every point along the length of the link is different. This generates an infinite degrees of freedom (DOF) model and is governed by nonlinear, coupled and partial differential equations (PDE). Then the model is discretized following the Euler Lagrangian technique in conjunction with an assumed mode approach (AMM).

Thus for TLFM, two dynamic models are developed. Initially using lumped parameter approach and thereafter by distributed parameter approach. These developed mathematical models of SLFM and TLFM, are used for designing controllers in subsequent Chapters.

2.2 Modeling of SLFM

The dynamics of the SLFM are developed in this section.

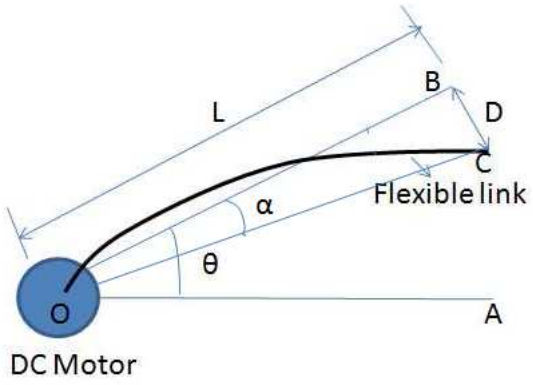

Figure 2.1: Schematic diagram of flexible link

Figure 2.1 shows a schematic diagram of a SFLM. The system consists of a single flexible link coupled to a DC motor shaft. The link is driven by a motor shaft and moves as per the input torque command provided by the DC motor. The shaft is coupled to the link through gear box having a certain gear ratio. Let the original position of the link be OA. When the motor shaft is actuated for an angle θ degrees from OA in the counter clockwise direction, it would have reached to new position OB, if it was a rigid link. However it is seen from the figure that due to the flexible nature the link, the link takes a shape given by OC. Therefore due to flexibility of the link, θ degrees at the motor hub results in a displacement of D at the end point. This generates an extra parameter called as tip deflection angle α due to flexibility. Angle α is assumed to be small therefore it can be approximated as

$$\alpha = \frac{D}{L},$$

where D is the displacement at the tip of the flexible link and L is the length of the link.

The various system parameters required for developing dynamic model of SLFM are listed below.

L : Length of link (m),

M : Mass of link (Kg),

f_c : Natural frequency (Hz),

J_l : Moment of inertia of link ($Kg\ m^2$),

J_{eq} : Equivalent moment of inertia of the hub ($Kg\ m^2$),

α : Tip deflection (deg),

V_m : DC input voltage (V),

I_m : Input current (A),

L_m : Motor armature inductance (H),

R_m : Motor armature resistance (Ohm),

E_{emf} : Equivalent back emf (V),

θ_m : Motor shaft position (deg),

K_m : Motor back emf constant (V s/deg),

J_m : Motor Inertia $(kg\ m^2)$,

T_m : Motor Torque (Nm),

T_l : Load Torque (Nm),

η_g : Gearbox efficiency,

K_g : Total gear ratio,

θ : Position of load angle (deg),

B_{eq} : Viscous damping coefficient,

η_m : Motor efficiency,

K_t : Motor torque constant (Nm/A),

K_s : Total stiffness of model (Nm/deg).

Following assumptions are made while developing a dynamic model:

- The link is long and slender hence shear and rotary inertia effects are negligible.
- Link moves in the horizontal direction only so it is not affected by gravity.
- It is rigidly clamped to the hub.

In controlling the tip of the link, it is sufficient to use a simplified model that will adequately describe the motion of the endpoint. Therefore the flexible link is assumed as a rotatory spring which is characterized by an equation,

$$J_l\ddot{\alpha} \quad = \quad -K_s\alpha \tag{2.1}$$

K_s can be estimated by measuring damped natural frequency ω_c for some known initial condition of α using the relation,

$$\ddot{\alpha} \quad = \quad -\omega_c^2\alpha, \tag{2.2}$$

Combining (2.1) and (2.2), we get

$$K_s = \omega_c^2 J_l$$

The link is modeled as a mass spring system having stiffness K_s and mass M and rotating about the axis at a distance L with moment of inertia,

$$J_l = \frac{ML^2}{3}$$

The potential energy of the system is,

$$U = P.E. = \frac{1}{2} K_s \alpha^2 \tag{2.3}$$

The total kinetic energy of the FLM is due to motion of the joint and the link.

KE due to hub is given as

$$T_h = \frac{1}{2} J_{eq} \dot{\theta}^2$$

where, $J_{eq} = J_l + \eta_g K_g^2 J_m$.

KE due to the link is given as

$$T_l = \frac{1}{2} J_l (\dot{\theta} + \dot{\alpha})^2$$

Therefore total KE of the system is given as

$$T = T_h + T_l = \frac{1}{2} J_{eq} \dot{\theta}^2 + \frac{1}{2} J_l (\dot{\theta} + \dot{\alpha})^2 \tag{2.4}$$

The Lagrangian of the system is $L = T - U$

Substituting values of U and T from (2.3) and (2.4)

$$L = \frac{1}{2} J_{eq} \dot{\theta}^2 + \frac{1}{2} J_l (\dot{\theta} + \dot{\alpha})^2 - \frac{1}{2} K_s \alpha^2 \tag{2.5}$$

The two generalized co-ordinates are α and θ. The Euler-Lagrange formulation is used to get the dynamical equations of the system as described below:

$$\frac{d}{dt}\left(\frac{\partial L}{\partial \dot{\theta}}\right) - \frac{\partial L}{\partial \theta} = T_l - B_{eq}\dot{\theta} \tag{2.6}$$

$$\frac{d}{dt}\left(\frac{\partial L}{\partial \dot{\alpha}}\right) - \frac{\partial L}{\partial \alpha} = 0. \tag{2.7}$$

Substituting L from (2.5) and solving (2.6) and (2.7), we get

$$J_{eq}\ddot{\theta} + J_l(\ddot{\theta} + \ddot{\alpha}) = T_l - B_{eq}\dot{\theta} \tag{2.8}$$

$$K_s\alpha + J_l(\ddot{\theta} + \ddot{\alpha}) = 0 \tag{2.9}$$

Rearranging the above equations,

$$\ddot{\theta} = \frac{T_l}{J_{eq}} - \frac{B_{eq}\dot{\theta}}{J_{eq}} + \frac{K_s\alpha}{J_{eq}} \tag{2.10}$$

$$\ddot{\alpha} = -K_s\left(\frac{1}{J_{eq}} + \frac{1}{J_l}\right)\alpha + \frac{B_{eq}}{J_{eq}}\dot{\theta} - \frac{T_l}{J_{eq}} \tag{2.11}$$

(2.10) and (2.11) represent dynamic equation of flexible link.

Actuator Model

DC motor is used to generate the necessary torque. The schematic is shown in Figure 2.2.

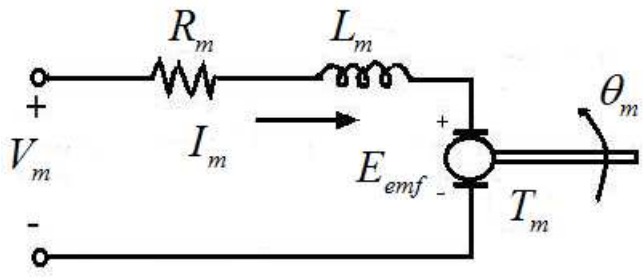

Figure 2.2: DC Motor: Equivalent circuit

Kirchhoff's Voltage law is used to get,

$$V_m - R_m I_m - L_m\frac{dI_m}{dt} - E_{emf} = 0.$$

Since, $L_m << R_m$, the motor inductance can be neglected, therefore,

$$I_m = \frac{V_m - E_{emf}}{R_m}. \tag{2.12}$$

The back emf generated by the motor is proportional to the motor shaft velocity i.e. $E_{emf} = K_m\dot{\theta}_m$. Therefore (2.12) can be written as below.

$$I_m = \frac{V_m - K_m\dot{\theta_m}}{R_m}, \tag{2.13}$$

where $\dot{\theta_m} = \omega_m$. Considering the mechanical aspect of the motor and applying Newton's 2nd law of motion to the motor shaft,

$$J_m\ddot{\theta_m} = T_m - \frac{T_l}{\eta_g K_g}, \tag{2.14}$$

here, $\theta_m = K_g\theta$ and $T_m = \eta_m K_t I_m$.

Substituting the value of T_m and θ_m in (2.14) and (2.13),

$$I_m = \frac{V_m - K_m K_g \dot{\theta}}{R_m} \tag{2.15}$$

$$J_m K_g \ddot{\theta} = \eta_m K_t I_m - \frac{T_l}{\eta_g K_g} \tag{2.16}$$

Substituting the value of (2.15) in (2.16)

$$J_m K_g \ddot{\theta} = \eta_m K_t \left(\frac{V_m - K_m K_g \dot{\theta}}{R_m} \right) - \frac{T_l}{\eta_g K_g} \tag{2.17}$$

Rearranging (2.17),

$$T_l = \eta_g \eta_m K_t K_g \left(\frac{V_m - K_m K_g \dot{\theta}}{R_m} \right) - J_m \eta_g K_g^2 \ddot{\theta}. \tag{2.18}$$

Further substituting (2.18) in (2.10) and (2.11), the following equations are obtained.

$$\ddot{\theta} = -p_1 \dot{\theta} + p_2 \alpha + p_3 V_m \tag{2.19}$$

$$\ddot{\alpha} = p_1 \dot{\theta} - p_4 \alpha - p_3 V_m \tag{2.20}$$

where the system parameters are defined as

$$\begin{aligned} p_1 &= \frac{\eta_g \eta_m K_t K_m K_g^2 + B_{eq} R_m}{(J_{eq} + J_m K_g^2 \eta_g) R_m} \\ p_2 &= \frac{K_s}{J_{eq} + J_m K_g^2 \eta_g} \\ p_3 &= \frac{\eta_g \eta_m K_t K_g}{(J_{eq} + J_m K_g^2 \eta_g) R_m} \\ p_4 &= \frac{K_s (J_l + Jeq + J_m K_g^2 \eta_g)}{J_{link} (J_{eq} + J_m K_g^2 \eta_g)}. \end{aligned}$$

Defining $x_1 = \theta$, $x_2 = \alpha$, $x_3 = \dot{\theta}$, $x_4 = \dot{\alpha}$ as the states and $V_m = u$, the dynamic model of the SLFM is represented in a state space form as,

$$\begin{aligned} \dot{x}_1 &= x_3 \\ \dot{x}_2 &= x_4 \\ \dot{x}_3 &= p_2 x_2 - p_1 x_3 + p_3 u \\ \dot{x}_4 &= -p_4 x_2 + p_1 x_3 - p_3 u. \\ y &= x_1 \end{aligned}$$

The system can be written as,

$$\begin{aligned} \dot{\mathbf{x}} &= A\mathbf{x} + \mathbf{b}u \\ y &= \mathbf{c}\,\mathbf{x} \end{aligned} \tag{2.21}$$

where $\mathbf{x} \in \mathbb{R}^{4\times1}$, $A \in \mathbb{R}^{4\times4}$, $\mathbf{b} \in \mathbb{R}^{4\times1}$, $\mathbf{c} \in \mathbb{R}^{1\times4}$.

$$A = \begin{bmatrix} 0 & 0 & 1 & 0 \\ 0 & 0 & 0 & 1 \\ 0 & p_2 & -p_1 & 0 \\ 0 & -p_4 & p_1 & 0 \end{bmatrix} \quad \mathbf{b} = \begin{bmatrix} 0 \\ 0 \\ p_3 \\ -p_3 \end{bmatrix} \quad \mathbf{c} = \begin{bmatrix} 1 & 0 & 0 & 0 \end{bmatrix}$$

This gives the mathematical model of SLFM system.

The plant under consideration is described in the following section.

2.3 Laboratory Set-up of SLFM Plant

This section describes the hardware equipment and software tools of laboratory set-up of SLFM. The SLFM plant from Quanser is shown in Figure 2.3. It consists of a flexible link coupled to a DC motor.

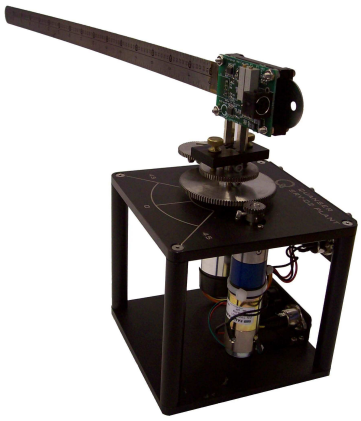

Figure 2.3: Plant of SLFM system

The various components are described below

- SLFM- It consists of a flexible link actuated by DC motor.
- Sensors- Potentiometer to measure the shaft angular displacement and strain gauge to measure the tip deflection. Both are placed at the base of each link.

The actual experimental set up with computer interface is shown in Figure 2.4.

Figure 2.4: Experimental set up of single flexible link

The system includes a single flexible link coupled to a DC motor, power supply for the DC motor, Data acquisition and control board, Sensors and Computer system with Matlab software. Wincon interfaces Matlab/Simulink with the Quanser Q4 board for implementing designed control of FLM system. Various parameters of the setup are listed in Table 2.1

Table 2.1: Physical parameters of SLFM plant

S.No.	Parameters	Values
1	η_g	0.9
2	η_m	0.69
3	K_g	70
4	K_t	0.00767 (Nm/A)
5	K_m	0.00767(Vs/deg)
6	B_{eq}	$4 * 10^{-3}$
7	J_l	1.3978 $(kg\ m^2)$
8	J_{eq}	0.002 $(kg\ m^2)$
9	R_m	2.6 (ohm)
10	K_s	0.0057 (Nm/deg)

Substituting the parameters from Table2.1 in system equations (2.21), the system matrices are obtained as

$$A = \begin{bmatrix} 0 & 0 & 1 & 0 \\ 0 & 0 & 0 & 1 \\ 0 & 212.7091 & -19.6573 & 0 \\ 0 & -616.9655 & 19.6573 & 0 \end{bmatrix} \mathbf{b} = \begin{bmatrix} 0 \\ 0 \\ 34.6024 \\ -34.6024 \end{bmatrix}$$

The dynamic model of single link flexible manipulator is thus cast to be utilised further for control development.

2.4 Dynamic Model of TLFM

Since single link manipulators are inadequate to reach to farther distances and to cover bigger working environments, multi link manipulators are employed in many of the applications. This section describes the development of the dynamic model of a TLFM plant. The system consists of two flexible links connected in series and each actuated by its own drive system. The primary link is rigidly clamped to the first drive (shoulder) and carries at its end the second harmonic

drive (elbow) to which another flexible link is attached. A payload is added at the outer link while the hub inertias are included at the actuated joints.

2.4.1 Model by Decoupled Approach

Initially TLFM is modeled using decoupled approach. In this approach, both the links along with their hubs are treated as two independent single flexible links and both the drives are controlled independently. Figure 2.5 represents the schematic diagram of a TLFM plant.

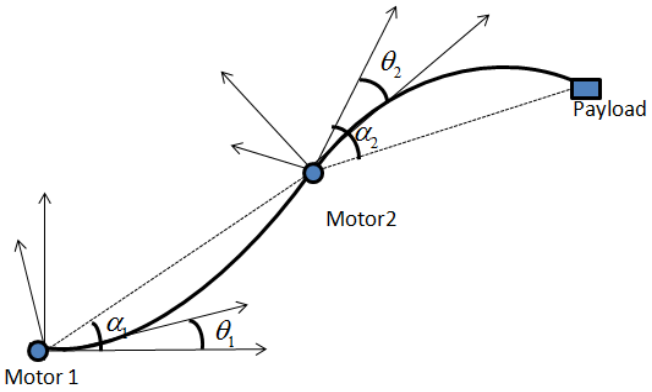

Figure 2.5: A planar two-link flexible manipulator

It is observed from Figure 2.5 that shoulder motor if actuated by an angle θ_1 in counterclockwise direction at the motor hub; results in a tip deflection α_1. Similarly, elbow motor displaced by an angle θ_2 in clockwise direction; results in a tip deflection of α_2 owing to the flexible nature of the links. Following are the parameters and constants of the plant:

α_i : Tip deflection (deg) of the link i

θ_i : Motor shaft position (deg) of i^{th} joint

T_{l_i} : Load Torque (Nm) of i^{th} link

B_{eq_i} : End-Effector Equivalent Viscous Damping Coefficient of i^{th} link

K_{s_i} : Torsional Stiffness Constant (Nm/deg) of i^{th} link

J_{l_i} and J_{eq_i} : Moment of inertia of i^{th} link and equivalent moment of inertia of the i^{th} stage.$(Kg\,m^2)$

$i = 1, 2$ for two links and two motors (motor 1 is a shoulder motor and motor 2 is an elbow

motor).

Following assumptions are made while developing a model of TLFM:

- Each link is long and slender hence shear and rotary inertia effects are negligible.
- The movement of each link is in the horizontal direction only, so it is not affected by gravity.
- Links are rigidly clamped to the hubs.

A decoupled approach is used neglecting the link coupling of the serial mechanism. The model of every flexible link is developed on similar lines as described in the previous section for SLFM. The dynamic equations of individual links are rewritten,

$$\ddot{\theta}_i = \frac{T_{l_i}}{J_{eq_i}} - \frac{B_{eq_i}\dot{\theta}_i}{J_{eq_i}} + \frac{K_{s_i}\alpha_i}{J_{eq_i}} \tag{2.22}$$

$$\ddot{\alpha}_i = -K_{s_i}\left(\frac{1}{J_{eq_i}} + \frac{1}{J_{l_i}}\right)\alpha_i + \frac{B_{eq_i}}{J_{eq_i}}\dot{\theta}_i - \frac{T_{l_i}}{J_{eq_i}} \tag{2.23}$$

for $i = 1, 2$.

Equivalent inertia of the hub includes the inertia of the links and end effector ahead. Stage 1 system includes shoulder motor and the first link.

Defining $x_{sh1} = \theta_1$, $x_{sh2} = \alpha_1$, $x_{sh3} = \dot{\theta}_1$, $x_{sh4} = \dot{\alpha}_1$ and $V_{m1} = u_1$, the system is represented in state space form as

$$\begin{aligned}
\dot{x}_{sh1} &= x_{sh3} \\
\dot{x}_{sh2} &= x_{sh4} \\
\dot{x}_{sh3} &= p_{2sh}x_{sh2} - p_{1sh}x_{sh3} + p_{3sh}u_1 \\
\dot{x}_{sh4} &= -p_{4sh}x_{sh2} + p_{1sh}x_{sh3} - p_{3sh}u_1.
\end{aligned}$$

where $p_{1sh}, p_{2sh}, p_{3sh}, p_{4sh}$ are parameters of the system.

It is represented in state space

$$\dot{\mathbf{x}}_{\mathbf{sh}} = A_1\mathbf{x}_{\mathbf{sh}} + \mathbf{b_1}u_1 \tag{2.24}$$

$$y_{sh} = \mathbf{c}_1\mathbf{x}_{sh}$$

$$\text{where, } A_1 = \begin{bmatrix} 0 & 0 & 1 & 0 \\ 0 & 0 & 0 & 1 \\ 0 & p_{2sh} & -p_{1sh} & 0 \\ 0 & -p_{4sh} & p_{1sh} & 0 \end{bmatrix} \quad \mathbf{x}_{sh} = \begin{bmatrix} x_{sh1} & x_{sh2} & x_{sh3} & x_{sh4} \end{bmatrix}^T$$

$$\mathbf{b}_1 = \begin{bmatrix} 0 \\ 0 \\ p_{3sh} \\ -p_{3sh} \end{bmatrix} \quad \mathbf{c}_1 = \begin{bmatrix} 1 & 0 & 0 & 0 \end{bmatrix}.$$

Stage 2 system includes the elbow motor and the second link. First link's equivalent moment of inertia is compounded with the stage 2 system. The dynamic equations are written on the similar lines of the stage 1 as follows.

Defining $x_{el1} = \theta_2$, $x_{el2} = \alpha_2$, $x_{el3} = \dot{\theta}_2$, $x_{el4} = \dot{\alpha}_2$ and $V_{m2} = u_2$ the system is represented in state space form as

$$\begin{aligned} \dot{x}_{el1} &= x_{el3} \\ \dot{x}_{el2} &= x_{el4} \\ \dot{x}_{el3} &= p_{2e}x_{el2} - p_{1e}x_{el3} + p_{3e}u_2 \\ \dot{x}_{el4} &= -p_{4e}x_{el2} + p_{1e}x_{el3} - p_{3e}u_2. \end{aligned}$$

where $p_{1e}, p_{2e}, p_{3e}, p_{4e}$ are system parameters. The equation is represented in state space form as

$$\begin{aligned} \dot{\mathbf{x}}_{\mathbf{el}} &= A_2\mathbf{x}_{\mathbf{el}} + \mathbf{b_2}u_2 \\ y_{el} &= \mathbf{c}_2\mathbf{x}_{el} \end{aligned} \tag{2.25}$$

$$\text{where, } A_2 = \begin{bmatrix} 0 & 0 & 1 & 0 \\ 0 & 0 & 0 & 1 \\ 0 & p_{2e} & -p_{1e} & 0 \\ 0 & -p_{4e} & p_{1e} & 0 \end{bmatrix} \quad \mathbf{x}_{el} = \begin{bmatrix} x_{el1} & x_{el2} & x_{el3} & x_{el4} \end{bmatrix}^T$$

$$\mathbf{b}_2 = \begin{bmatrix} 0 \\ 0 \\ p_{3e} \\ -p_{3e} \end{bmatrix} \quad \mathbf{c_2} = \begin{bmatrix} 1 & 0 & 0 & 0 \end{bmatrix}.$$

Thus the mathematical model for TLFM plant is cast using decoupled approach.

The TLFM plant under consideration is described in the following section.

2.5 Laboratory Set-up of TLFM Plant

The TLFM plant with its various components is shown in Figure 2.6.

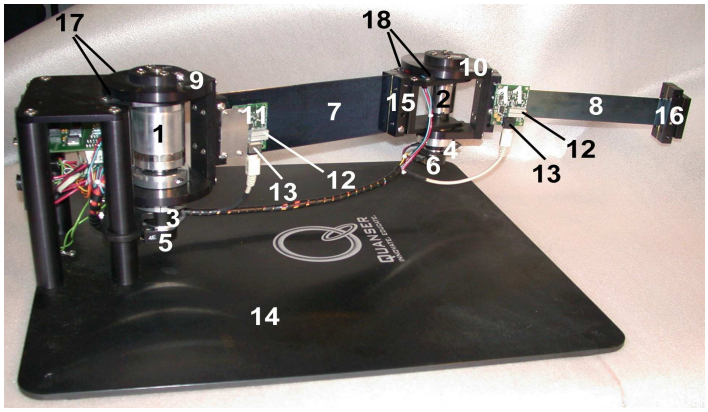

Figure 2.6: Plant of TLFM system

The various components are described below

- TLFM- It consists of two flexible links (7 and 8) connected in series and each actuated by its own drive system. The primary link is rigidly clamped to the first drive 1 (shoulder) and carries at its end the second harmonic drive 2(elbow) to which another flexible link is attached.
- Actuators- There are two DC motors (3 and 4) to actuate two links of the TLFM plant. The shoulder motor is actuated by an angle θ_1 at the motor hub and results in a tip deflection angle α_1 and elbow motor is displaced by an angle θ_2 and results in a tip deflection angle α_2 owing to the flexible nature of the links.
- Sensors- Two digital optical encoders (5 and 6) measure the shaft angular displacement and two strain gauges (11) to measure the tip deflection are placed at the base of each link.

Physical parameters of the TLFM plant are listed in Table 2.2.

Table 2.2: Physical Parameters of TLFM plant

Parameter	Link-1	$Link-2$
Link length	0.201m	0.2m
Elasticity	2.0684*10^{11}(N/m2)	2.0684*10^{11}(N/m2)
Rotor moment of Inertia	6.28*10-6 (kg m2)	1.03*10-6 (kg m2)
Drive moment of Inertia	7.361*10^{-4}(kg m2)	44.55*10^{-6}(kg m2)
Link moment of Inertia	0.17043 (kg m2)	0.0064387 (kg m2)
Gear ratio	100	50
Maximum Rotation	(+/-90, +/-90)deg.	(+/-90, +/-90)deg.
Drive Torque constant	0.119 (Nm/A)	0.0234 (Nm/A)

This plant is interfaced to computer using DAQ as shown in block schematics in Figure 2.7.

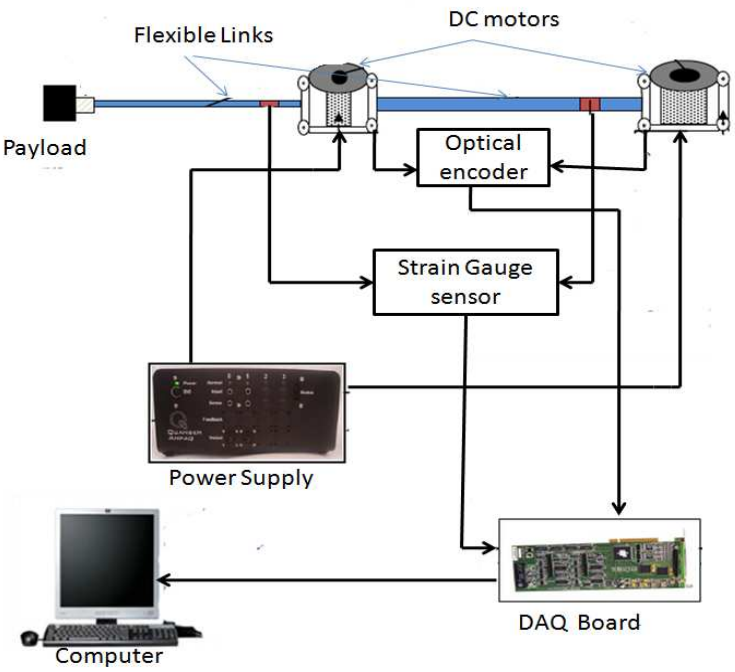

Figure 2.7: Block diagram

A Data acquisition board (DAQ) provides two Analog-to-Digital (A/D) and Digital-to-Analog (D/A)converters on board. All the signals from the sensors are interfaced to PC via this DAQ board. Similarly the control signals from the PC are connected to the actuators from this board. A Power supply is required for powering actuators and DAQ board along with PC. Quarc software establish the compatibility between Matlab and DAQ.

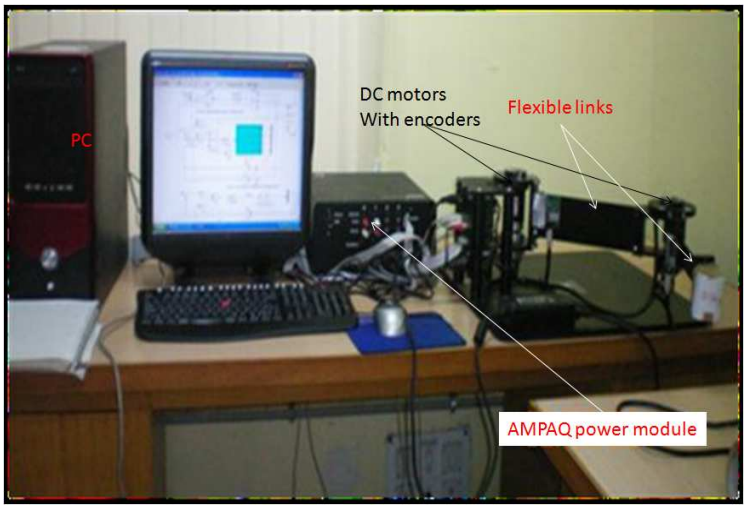

Figure 2.8: Experimental Setup of TLFM system

Complete experimental set up is shown in Figure 2.8.
This experimental set up is used for implementing various controllers developed for TLFM. Substituting values of various physical parameters of the plant from Table2.2, system matrices for shoulder system become

$$A_1 = \begin{bmatrix} 0 & 0 & 1 & 0 \\ 0 & 0 & 0 & 1 \\ 0 & 628.89 & -62.95 & 0 \\ 0 & -863.33 & 62.95 & 0 \end{bmatrix} \quad \mathbf{b}_1 = \begin{bmatrix} 0 \\ 0 \\ 140.47 \\ -140.47 \end{bmatrix} \quad \mathbf{c}_1 = \begin{bmatrix} 1 & 0 & 0 & 0 \end{bmatrix}.$$

After substituting the values of various system constants, system matrices for elbow system

become

$$A_2 = \begin{bmatrix} 0 & 0 & 1 & 0 \\ 0 & 0 & 0 & 1 \\ 0 & 2271.7 & -496.8 & 28.4 \\ 0 & -3336.2 & 496.8 & -41.6 \end{bmatrix} \quad \mathbf{b}_2 = \begin{bmatrix} 0 \\ 0 \\ 288.12 \\ -288.12 \end{bmatrix} \quad \mathbf{c}_2 = \begin{bmatrix} 1 & 0 & 0 & 0 \end{bmatrix}.$$

This model of TLFM plant is used in Chapter 6 for developing sliding mode controllers.

Model obtained by decoupled approach utilizes the lumped parametric method where the individual flexible link is approximated as a lumped mass and spring rotating about its axis. This results in an approximate model, since an actual flexible system has a distributed parametric nature. Two kinds of errors are introduced if the flexibility effect is not considered in the mathematical model. The first kind of error is introduced in the torque requirement for the motors and the second kind results in the positioning inaccuracy of the end-effector. Therefore to reduce the modeling errors, a distributed parametric approach along with assumed mode method (AMM) is studied for modeling TLFM plant. It is described in the following section.

2.5.1 Model using Assumed Mode Method

To achieve better control of a physical plant, one has to start with accurate mathematical model for the system. A good model of FLM must include its distributed nature due to flexibility. Energy based Lagrangian approach is more suitable for deriving the dynamic model of a flexible mechanical system having structural deformations [6]. A flexible manipulator is a continuous dynamic system, characterized by infinite number of degrees-of-freedom (DOF) and governed by nonlinear, coupled, partial differential equations (PDE). Exact solution of these equations is not feasible and infinite DOF model imposes several constraints on design of the controllers as well. Therefore the equations are made finite using numerical technique namely the AMM [2]. The AMM approach consists of representing the elastic displacement as a linear combination of spatial and time coordinates.

A dynamic model of a TLFM is derived adopting the Euler Lagrangian technique in conjunction with the assumed mode approach [6].

2.5.2 Kinematics of the Plant

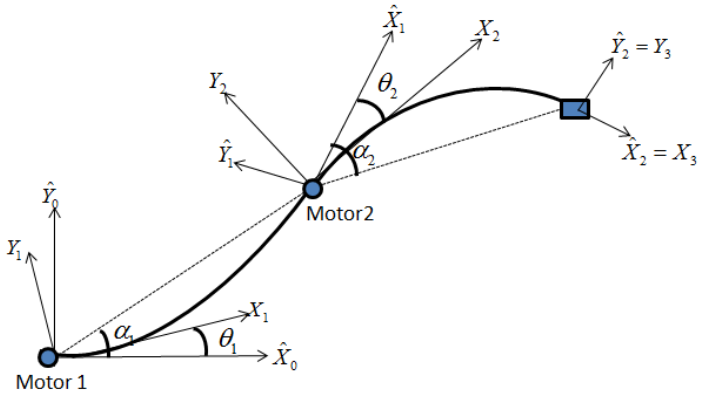

Figure 2.9: A schematic of two-link flexible manipulator

Figure 2.9 illustrates schematic representation of a planar 2-link flexible manipulator. It consists of 2 flexible links producing bending deformations only in the horizontal plane and has two rotary joints actuated by DC motors.
θ_i is the joint angle of the i^{th} joint and $y_i(x_i, t)$ represents the deflection along i^{th} link. The outer free end of the TLFM is attached with a payload of mass M_p.
The various frames of reference are

- $(\widehat{X}_0, \widehat{Y}_0)$: The inertial frame or fixed reference frame at the hub of the shoulder motor.
- (X_1, Y_1): The rigid body coordinate frame associate with the first link, which is also at the hub of the shoulder motor.
- $(\widehat{X}_1, \widehat{Y}_1)$: Moving co-ordinate frame at the end of the link 1 i.e. at the hub of the elbow motor.
- (X_2, Y_2): The rigid body coordinate frame associate with the second link,
- $(\widehat{X}_2, \widehat{Y}_2)$: Moving co-ordinate frame at the end of the link 2 i.e. at the payload, which is also (X_3, Y_3).

The rigid body motion is described by joint angle θ_i and transversal flexible motion of link i is given by $y_i(x_i, t)$.

The kinematics is developed using the transformation matrices. The deflection of the link i through a deflection angle θ_i is given using joint (rigid) rotation matrix A_{Ti} as

$$A_{Ti} = \begin{bmatrix} cos\theta_i & -sin\theta_i \\ sin\theta_i & cos\theta_i \end{bmatrix} \tag{2.26}$$

whereas the end-point of the flexible link is characterized using the rotation matrix $\mathbf{E}_i$ [80] as follows.

$$\mathbf{E}_i = \begin{bmatrix} 1 & -y'_{ie} \\ y'_{ie} & 1 \end{bmatrix}, \tag{2.27}$$

where

$$y'_{ie} = \frac{\partial y_i}{\partial x_i}|_{x_i=l_i}$$

l_i being the length of the link i.

Links subjected to bending store potential energy by virtue of their deflection and kinetic energy by virtue of their deflection rates.

Kinetic Energy

Any point on flexible link-1 can be described with co-ordinates $(x_1, y_1(x_1, t))$ with respect to the rigid body frame (X_i, Y_i). The transversal deformation $y_1(x_1, t)$ characterizes the flexible nature of the link which in turn is separated in space and time co-ordinates using AMM as

$$y_1(x_1, t) = \phi_1(x_1)\delta_1(t)$$

where $\delta_1(t)$ is the time varying generalized coordinate of the first link, and $\phi_1(x_1)$ is its spatial coordinates.

The rigid body frame in turn is obtained via rotation angle θ_1 from inertial frame $(\widehat{X}_0, \widehat{Y}_0)$ using rotation matrix A_{T1}. Therefore a point on the first flexible link can be described by a position vector $\mathbf{p}_1(x_1)$ w.r.t. inertial (absolute) frame and is given by

$$\mathbf{p}_1(x_1) = A_{T1} \begin{bmatrix} x_1 \\ y_1(x_1, t) \end{bmatrix} \tag{2.28}$$

The kinetic energy of link-1 is given as

$$T_{l1} = \frac{1}{2} \int_0^{l1} \rho_1(x_1)\dot{\mathbf{p}}_1^T(x_1)\dot{\mathbf{p}}_1(x_1)dx_1 \tag{2.29}$$

where ρ_1 is the linear mass density of link-1 in $[kg/m]$.

Any point on flexible link-2 is characterized as follows.

A point on link 1 is described as $(x_1, y_1(x_1,t))$. At the end of link 1 it becomes $(l_1, y_{1e})^T$, where l_1 is the length of link-1 and

$$y_{1e} = y_1(x_1,t)|_{x_1=l_1}$$

gives the deflection of link-1 at the tip.

The frame $(\widehat{X}_1, \widehat{Y}_1)$, which is the frame at the elbow motor, is described with respect to the rigid frame of link 1 (X_1, Y_1) as $(l_1 \ \ y_{1e})^T$. It is related w.r.t inertial frame $(\widehat{X}_0, \widehat{Y}_0)$ as $A_{T1}(l_1 \ \ y_{1e})^T$. $(\widehat{X}_1, \widehat{Y}_1)$ is the reference frame for link-2. The rigid body frame for link-2 (X_2, Y_2) is obtained from the reference frame $(\widehat{X}_1, \widehat{Y}_1)$ via rotation angle θ_2 using rotation matrix A_{T2}. Any point on flexible link-2 can be described with co-ordinates $(x_2, y_2(x_2,t))$.

The transversal deformation

$$y_2(x_2,t) = \phi_2(x_2)\delta_2(t),$$

where $\delta_2(t)$ is the time varying generalized coordinate of the second link, and $\phi_2(x_2)$ is its spatial coordinates.

Any point on link-2 is described w.r.t $(\widehat{X}_1, \widehat{Y}_1)$ as $A_{T2}(x_2 \ \ y_2(x_{l2},t))^T$.

Since $(\hat{X}_1, \hat{Y}_1)$ is related w.r.t.the inertial frame $(\widehat{X}_0, \widehat{Y}_0)$ with position vector of $A_{T1}(l_1 \ \ y_{1e})^T$, any point on link-2 is described by a position vector $\mathbf{p_2}(\mathbf{x_2})$ and is given by

$$\mathbf{p}_2(x_2) = A_{T1} \begin{bmatrix} l_1 \\ y_{1e} \end{bmatrix} + A_{T1}\mathbf{E}_1 A_{T2} \begin{bmatrix} x_2 \\ y_2(x_2,t) \end{bmatrix} \tag{2.30}$$

Kinetic energy due to link-2 is given as

$$T_{l2} = \frac{1}{2}\int_0^{l2} \rho_2(x_2)\dot{\mathbf{p}}_2^T(x_2)\dot{\mathbf{p}}_2(x_2)dx_{l2} \tag{2.31}$$

where ρ_2 is the linear mass density of link-2 in $[kg/m]$.

To calculate the kinetic energy due to the hubs and the payload, their co-ordinates with respect to the inertial frame have to be described. Their position vectors are given below.

$\mathbf{r_1}$ describes the position vector for joint 1. Since joint 1 lies at the inertial frame,

$$\mathbf{r}_1 = [0 \ \ 0]^T$$

$\mathbf{r_2}$ describes the position vector for joint 2 from the inertial frame.

Joint 2 lies at the frame $(\hat{X}_1, \hat{Y}_1)$, therefore as described above the relative position of $(\hat{X}_1, \hat{Y}_1)$

from the inertial frame is described as

$$\mathbf{r}_2 = A_{T1}[l_1 \;\; y_{1e}]^T$$

Let the position vector characterizing the payload from the inertial frame be $\mathbf{r_3}$. Any point on the flexible link-2 is described by a position vector $\mathbf{p_2}(\mathbf{x_2})$ and payload is at the end of the second link. Therefore in the expression of $\mathbf{p_2}(\mathbf{x_2})$, $(x_2, y_2(x_2))$ is to be replaced by (l_2, y_{2e}), giving the absolute position of the payload w.r.t.inertial frame as

$$\mathbf{r}_3 = A_{T1}[l_1 \;\; y_{1e}]^T + A_{T1}\mathbf{E}_1 A_2[l_2 \;\; y_{2e}]^T$$

With these kinematics, any point on the TLFM system is completely characterized.

Velocity vectors of the hubs and payload are given by differentiating the corresponding position vectors.

The tip angles for the links namely α_1 and α_2 are approximated as

$$\begin{aligned} \alpha_1 &= \theta_1 + y_{1e} \\ \alpha_2 &= (\theta_1 + y_{1e}) + (\theta_2 + y_{2e}) \end{aligned}$$

For the plant under consideration, there are two hubs.

Kinetic energy due to joints (hubs) is $T_h = T_{h1} + T_{h2}$,

where T_{h1} is the kinetic energy due to joint 1 of mass m_{h1} and is given as

$$T_{h1} = \frac{1}{2} m_{h1} \dot{\mathbf{r}}_1^T \dot{\mathbf{r}}_1 + \frac{1}{2} J_{h1} \dot{\alpha_1}^2 \tag{2.32}$$

and T_{h2} is the kinetic energy due to joint 2 of mass m_{h2}, given as

$$T_{h2} = \frac{1}{2} m_{h2} \dot{\mathbf{r}}_2^T \dot{\mathbf{r}}_2 + \frac{1}{2} J_{h2} \dot{\alpha_2}^2 \tag{2.33}$$

where J_{h1} and J_{h2} are the hub inertia of joint 1,2 respectively in kgm^2.

T_p is the KE of the payload, which is connected at the end of the second link and is given as

$$T_p = \frac{1}{2} m_p \dot{\mathbf{r}}_3^T \dot{\mathbf{r}}_3 + \frac{1}{2} J_p (\dot{\alpha}_2 + \dot{y}'_{2e})^2 \tag{2.34}$$

where J_p and m_p are the moment of inertia and mass of the payload. The total kinetic energy of the flexible link manipulator is due to motions of joints, links and payload. By adding all the above corresponding equations, total kinetic energy can be calculated. Thus the total KE of the plant is given as

$$T = T_{h1} + T_{h2} + T_{l1} + T_{l2} + T_p \tag{2.35}$$

Potential Energy

The potential energy (PE) of the FLM arises from deformation of the links. In absence of gravity (horizontal plane motion) PE is stored in both the links and is given as

$$U = PE_1 + PE_2 \tag{2.36}$$

where

$$PE_1 = \frac{1}{2}\int_0^{l1} (EI)_1(x_1)\Big[\frac{d^2y_1(x_1)}{dx_1^2}\Big]^2 dx_1 \tag{2.37}$$

is the PE of the first link, and

$$PE_2 = \frac{1}{2}\int_0^{l2} (EI)_2(x_2)\Big[\frac{d^2y_2(x_2)}{dx_2^2}\Big]^2 dx_2 \tag{2.38}$$

is the PE of the second link. Here E_i is youngs modulus of link i in N/m^2 and I_i is the second moment of inertia of link i in kgm^2 and $(EI)_i$ is the constant flexural rigidity of the link.
Now the Lagrangian can be formed substituting the kinetic and potential energy from (2.35) and (2.36) as $L = T - U$.

2.5.3 Flexible Link Modeling

The links are modeled as Euler-Bernoulli beams with clamped-mass boundary conditions. The deflection $y_i(x_i, t)$ of the i^{th} link, at a distance x_i from the frame placed at the i^{th} joint, satisfies the following partial differential equation [2].

$$(EI)_i\frac{\partial^4 y_i(x_i,t)}{\partial x_i^4} + \rho_i\frac{\partial^2 y_i(x_i,t)}{\partial t^2} = 0, i = 1, 2 \tag{2.39}$$

where n = number of links and ρ_i is uniform density of the link respectively.
To solve this equation, following boundary conditions are imposed at the base of each link.

$$y_i(0,t) = 0, y_i{}'(0,t) = 0, i = 1, 2 \tag{2.40}$$

Other two boundary conditions are given by balancing the moment and shearing force at the end of the link as

$$(EI)_i\frac{\partial^2 y_i(x_i,t)}{\partial x_i^2}\Big|_{x_i=l_i} = -J_{Li}\frac{d^2}{dt^2}\Big(\frac{\partial^2 y_i(x_i,t)}{\partial x_i^2}\Big)\Big|_{x_i=l_i} \tag{2.41}$$

and

$$(EI)_i \frac{\partial^3 y_i(x_i,t)}{\partial x_i^3}\Big|_{x_i=l_i} = M_{Li}\frac{d^2}{dt^2}(y_i(x_i,t))|_{x_i=l_i} \tag{2.42}$$

where M_{Li}, and J_{Li} are the mass and moment of inertia at the end of link i. There can be infinite solutions for equation (2.39) generating an infinite DOF model which is limited to finite dimensions using Assumed Mode technique.

Assumed Mode Technique

Finite dimensional discretization for link deflection can be obtained by the method of separation of variables [6], giving

$$y_i(x_i,t) = \sum_{j=1}^{m_i} \phi_{ij}(x_i)\delta_{ij}(t), i = 1,2 \tag{2.43}$$

where, m_i = number of flexible variables used to describe the link deformation. $\delta_{ij}(t)$ are the time varying generalized coordinates of the i^{th} link, and $\phi_{ij}(x_i)$ are its spatial coordinates. For the plant under study, 2 flexible modes are considered per link. Therefore $m_i = 2$.
Mode Eigen function $\phi_{ij}(x_i)$ satisfying clamped mass boundary conditions with Euler Bernoulli beam theory for bending vibrations is given as [81]

$$\phi_{ij}(x_i) = C_{1,ij}sin(\beta_{ij}x_i) + C_{2,ij}cos(\beta_{ij}x_i) + C_{3,ij}sinh(\beta_{ij}x_i) + C_{4,ij}cosh(\beta_{ij}x_i) \tag{2.44}$$

where, $C_{1,ij}, C_{2,ij}, C_{3,ij}, C_{4,ij}$ are positive constants and β_{ij} are the Eigen values. The solution for time varying coordinate $\delta_{ij}(t)$ is given as [6]

$$\delta_{ij} = exp(j\omega_{ij}t) = C_{5,ij}sin(\omega_{ij}t) + C_{6,ij}cos(\omega_{ij}t) \tag{2.45}$$

Constants $C_{1,ij}.....C_{6,ij}$ are obtained from the boundary conditions (2.40), (2.41) and (2.42).
From (2.40), we get $C_{3,ij} = -C_{1,ij}$ and $C_{4,ij} = -C_{2,ij}$.
Substituting $\phi_{ij}(x_i)$ from (2.44) in (2.43), expression of deflection $y_i(x_i,t)$ is obtained with constants $C_{1,ij}$ and $C_{2,ij}$. This $y_i(x_i,t)$ is substituted in the boundary conditions imposed by (2.41) and (2.42). It leads to a homogeneous equation of the following form.

$$F\begin{bmatrix} C_{1ij} \\ C_{2ij} \end{bmatrix} = 0$$

$F \in \mathbb{R}^{(2\times 2)}$ and is a function of β_{ij}. Solutions of this equation gives the values of β_{ij}. Since, constants C_{1ij} and C_{2ij} are non-zero, the determinant F has to be zero. This gives the following transcendental equation [82].

$$\begin{aligned} & (1 + cos(\beta_{ij}l_i)cosh(\beta_{ij}l_i)) - \frac{M_{Li}\beta_{ij}}{\rho_i}(sin(\beta_{ij}l_i)cosh(\beta_{ij}l_i) - cos(\beta_{ij}l_i)sinh(\beta_{ij}l_i)) \\ - & \frac{J_{Li}\beta_{ij}^3}{\rho_i}(sin(\beta_{ij}l_i)cosh(\beta_{ij}l_i) + cos(\beta_{ij}l_i)sinh(\beta_{ij}l_i)) \\ + & \frac{M_{Li}J_{Li}\beta_{ij}^4}{\rho_i^2}(1 - cos(\beta_{ij}l_i)cosh(\beta_{ij}l_i) = 0 \end{aligned} \tag{2.46}$$

β_{ij} are found out from (2.46). It is observed that only the known physical parameters of the links are required to get the values of β_{ij}. For link-1, first two positive roots of this equation give β_{11}, β_{12}.

j^{th} natural frequency of i^{th} link ω_{ij} is obtained using

$$\beta_{ij}^4 = \omega_{ij}^2\rho_i/(EI)_i \tag{2.47}$$

Similar procedure is followed for link-2. This shows that β_{ij} is dependent only on the physical properties of the link. Using these values of β_{ij}, values of $C_{1,ij}$ and $C_{2,ij}$ are calculated through a normalization [9],

$$\int_0^{li} [\phi_{ij}(x_i)]^2 dx_i = l_i.$$

Substituting ϕ_{ij} from (2.44) and δ_{ij} from (2.45), PDE described by (2.39) can be separated in space and time. These illustrations are used to get exact expression of potential energy and hence Lagrangian. Now the generalized coordinates are selected to solve the Lagrangian formed in the previous section. For our plant, there are 2 links and we have selected 2 modes per link. Therefore the Lagrangian $L = T - U$ now becomes a function of 6 generalized coordinates namely $\theta_1, \theta_2, \delta_{11}, \delta_{12}, \delta_{21}, \delta_{22}$. Then the motion equations of TLFM robot arm are formed by the following Euler-Lagrange equations.

$$\frac{d}{dt}\left(\frac{\partial L}{\partial \dot{q}}\right) - \frac{\partial L}{\partial q} = \tau_i, i = 1, 2$$

where $\boldsymbol{q} = (\boldsymbol{q_r}^T \ \boldsymbol{q_f}^T)^T$.

$\boldsymbol{q}_r$ represents generalized coordinates for rigid variables $\boldsymbol{\theta}$ and $\boldsymbol{q}_f$ represents generalized coordinates for flexible variables $\boldsymbol{\delta}$. Hence we can write $\boldsymbol{q} = (\boldsymbol{\theta}^T \ \boldsymbol{\delta}^T)^T$. The force corresponding to joint variable $\boldsymbol{q}_r$ is the joint input torque τ_i and for flexible deformation variables $\boldsymbol{q}_f$ the

corresponding force is zero. For clamped condition, there is no elastic displacement at the joints [9], [16]. The general form of Lagrange's equation for clamped case is then,

- for joint variables,
$$\frac{d}{dt}\left(\frac{\partial L}{\partial \dot{\theta}_i}\right) - \frac{\partial L}{\partial \theta_i} = \tau_i, i = 1, 2$$
where τ_i is the torque developed at joint i.
For the system with two links, we get
$$\frac{d}{dt}\left(\frac{\partial L}{\partial \dot{\theta}_1}\right) - \frac{\partial L}{\partial \theta_1} = \tau_1$$
$$\frac{d}{dt}\left(\frac{\partial L}{\partial \dot{\theta}_2}\right) - \frac{\partial L}{\partial \theta_2} = \tau_2$$

- for flexible variables,
$$\frac{d}{dt}\left(\frac{\partial L}{\partial \dot{\delta_{ij}}}\right) - \frac{\partial L}{\partial \delta_{ij}} = 0, j = 1....m_i, i = 1, 2$$
We have 2 flexible modes per link. Hence we can write,

  1. for first link,
$$\frac{d}{dt}\left(\frac{\partial L}{\partial \dot{\delta_{11}}}\right) - \frac{\partial L}{\partial \delta_{11}} = 0,$$
$$\frac{d}{dt}\left(\frac{\partial L}{\partial \dot{\delta_{12}}}\right) - \frac{\partial L}{\partial \delta_{12}} = 0$$
  2. for second link,
$$\frac{d}{dt}\left(\frac{\partial L}{\partial \dot{\delta_{21}}}\right) - \frac{\partial L}{\partial \delta_{21}} = 0,$$
$$\frac{d}{dt}\left(\frac{\partial L}{\partial \dot{\delta_{21}}}\right) - \frac{\partial L}{\partial \delta_{22}} = 0$$

These 6 equations are arranged to give a familiar closed form of equation of motion.

2.5.4 Closed form Equation of Motion

Symbolic closed form of equations are most effective to implement real time control algorithms for controlling FLM [83], [84]. As a result of this procedure, the equation of motion for a TLFM

can be written in a familiar closed form as

$$\begin{bmatrix} B_1(\theta_i,\delta_{ij}) & B_2(\theta_i,\delta_{ij}) \\ B_3(\theta_i,\delta_{ij}) & B_4(\theta_i,\delta_{ij}) \end{bmatrix} \begin{bmatrix} \ddot{\theta}_i \\ \ddot{\delta_{ij}} \end{bmatrix} + \begin{bmatrix} h_1(\theta_i,\delta_{ij},\dot{\theta}_i,\dot{\delta_{ij}}) \\ h_2(\theta_i,\delta_{ij},\dot{\theta}_i,\dot{\delta_{ij}}) \end{bmatrix}$$
$$+K \begin{bmatrix} 0 \\ \delta_{ij} \end{bmatrix} + D \begin{bmatrix} 0 \\ \dot{\delta_{ij}} \end{bmatrix} = \begin{bmatrix} I \\ 0 \end{bmatrix} \tau_i \tag{2.48}$$

where

τ_i : Actuated torque of the i^{th} link (i = 1, 2).

$\theta_i, \dot{\theta}_i$: Joint angle and velocity of the i^{th} joint.

$\delta_{ij}, \dot{\delta_{ij}}$: Modal displacement and velocity of the i^{th} link.

B : A positive definite symmetric inertia matrix partitioned according to the joint (rigid) and link (flexible) coordinates as $B_1 \in \mathbb{R}^{(2\times2)}$, $B_2 \in \mathbb{R}^{(2\times4)}$, $B_3 \in \mathbb{R}^{(4\times2)}$ and $B_4 \in \mathbb{R}^{(4\times4)}$.

$\mathbf{h_1} \in \mathbb{R}^{(\mathbf{2\times1})}, \mathbf{h_2} \in \mathbb{R}^{(\mathbf{4\times1})}$: Vectors containing Coriolis and centrifugal forces which can be computed via the Christoffel symbols, [85] i.e., via differentiation of the inertia matrix elements. Each component of these terms is a quadratic form in the velocity vector $(\dot{\boldsymbol{\theta}}\ \dot{\boldsymbol{\delta}})$.

K : Diagonal stiffness matrix

D : Damping matrix.

$I \in \mathbb{R}^{(2\times2)}$ is an identity matrix.

0 is a zero matrix of appropriate dimensions.

$B(\mathbf{q})$ and $\mathbf{h}(\mathbf{q}, \dot{\mathbf{q}})$ are further represented as simply B and $\mathbf{h}$ for notational simplicity in the subsequent equations. Therefore equation (2.48) can be written as

$$\begin{aligned} B_1\ddot{\boldsymbol{\theta}} + B_2\ddot{\boldsymbol{\delta}} + \mathbf{h_1} &= \boldsymbol{\tau_i} \\ B_3\ddot{\boldsymbol{\theta}} + B_4\ddot{\boldsymbol{\delta}} + K\boldsymbol{\delta} + D\dot{\boldsymbol{\delta}} + \mathbf{h_2} &= \mathbf{0} \end{aligned} \tag{2.49}$$

This represents closed form of motion equations. For TLFM system substituting the parameters from Table 2.2, various system matrices become

$$B_1 = \begin{pmatrix} 0.6171 & 0.1713 \\ 0.1713 & 0.1338 \end{pmatrix}, \qquad B_2 = \begin{pmatrix} 0.2401 & 0.0532 & 0.1181 & 0.0307 \\ 0.1018 & -0.0588 & 0.0575 & 0.0071 \end{pmatrix}$$

$$B_3 = \begin{pmatrix} 0.2401 & 0.1018 \\ 0.0532 & -0.0588 \\ 0.1181 & 0.0575 \\ 0.0307 & 0.0071 \end{pmatrix}, \qquad B_4 = \begin{pmatrix} 0.1183 & 0.0028 & 0.0603 & 0.0134 \\ 0.0028 & 0.0819 & -0.0061 & 0.0061 \\ 0.0603 & -0.0061 & 0.1000 & 0 \\ 0.0134 & 0.0061 & 0 & 0.1000 \end{pmatrix}$$

$$h_1 = \begin{pmatrix} -0.2807 \\ 0.0217 \end{pmatrix}, \qquad h_2 = \begin{pmatrix} -0.0983 \\ -0.1423 \\ 0.0351 \\ 0.0136 \end{pmatrix}$$

$$K = \begin{pmatrix} 0.9096 & 0 & 0 & 0 \\ 0 & 12.7910 & 0 & 0 \\ 0 & 0 & 18.7617 & 0 \\ 0 & 0 & 0 & 999.3097 \end{pmatrix}, \; D = \begin{pmatrix} 0.0954 & 0 & 0 & 0 \\ 0 & 0.3576 & 0 & 0 \\ 0 & 0 & 0.4331 & 0 \\ 0 & 0 & 0 & 3.1612 \end{pmatrix}$$

This model of TLFM using AMM approach is used for developing control in Chapter 6.

2.6 Model Validation of TLFM

To validate the correctness of the dynamic model derived in the previous section, model validation is carried out. The mathematical model is excited with a particular input signal in simulation and the response of the model is stored. Then the same input is used in experiment to excite the plant and its response is noted. These open-loop responses of both actual physical plant and derived model of the TLFM are compared. The procedure is repeated for various types of input signals.

2.6.1 Model Validation Results and Discussions

To analyze the open loop response of the developed mathematical model of the TLFM, numerical simulation has been performed using MATLAB/SIMULINK software. Now different input torques are applied to both the joints. Pulse type torque profiles are applied to both the motors of the TLFM for simulated model and in experiment as shown in Figure 2.10. The torque profile for both joint-1 and joint-2 has amplitude of 0.42 Nm.

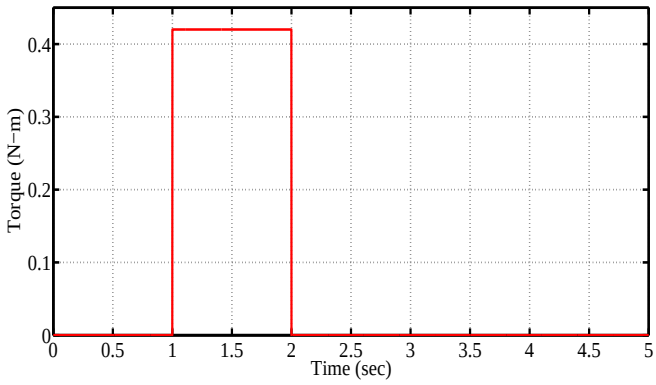

Figure 2.10: Pulse input

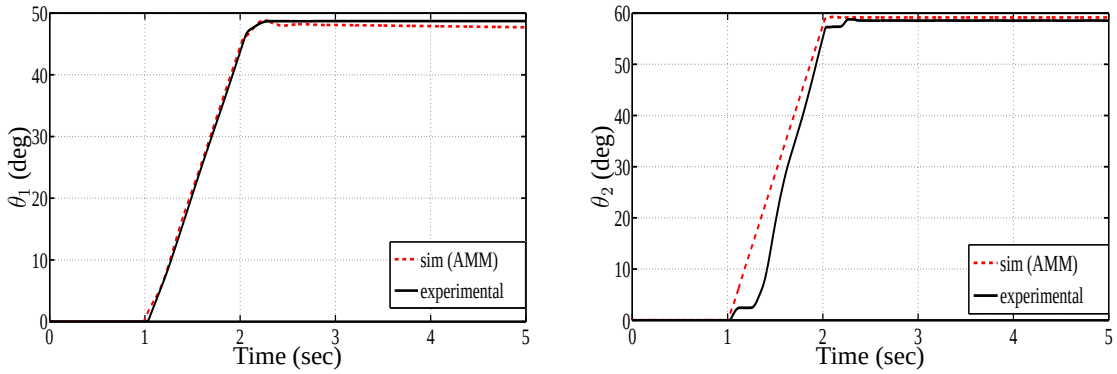

(a) Motor 1 (b) Motor 2

Figure 2.11: Response to pulse input

Figure 2.11(a) shows the response of motor-1 to the applied torque input. It shows a maximum amplitude of 48° for both the simulated and experimental model. They are in close agreement verifying the correctness of the model. The joint-2 position response is shown in Figure 2.11(b). The maximum deflection for joint-2 is observed to be 59° for both the models. Deflection for joint-2 is more than that of joint-1 since joint-1 is clamped and joint-2 is pinned. Joint-2 is attached at the end of the first flexible link and also the joint flexibility is neglected. Therefore Figure 2.11(b) shows that during the rise time, there is a little mismatch in the response for θ_2 in experiment and in simulation.

To further validate the proposed model, square torque signals are applied to both the actuators. Square torque signal is chosen as it excites all the flexible modes as well as coupling terms. A

square wave signal shown in Figure 2.12, with amplitude 0.2 N-m and frequency of 1 Hz is applied to joint-1 and joint-2.

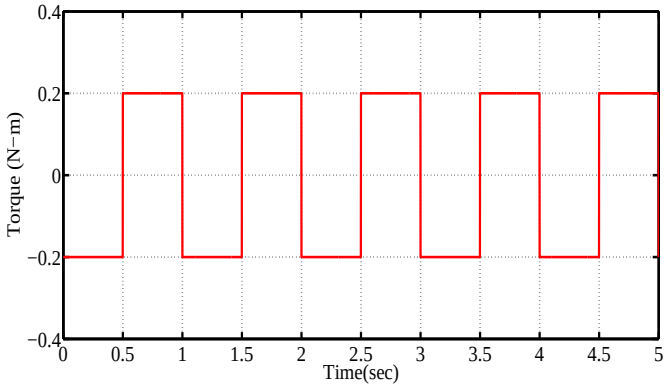

Figure 2.12: Square wave input

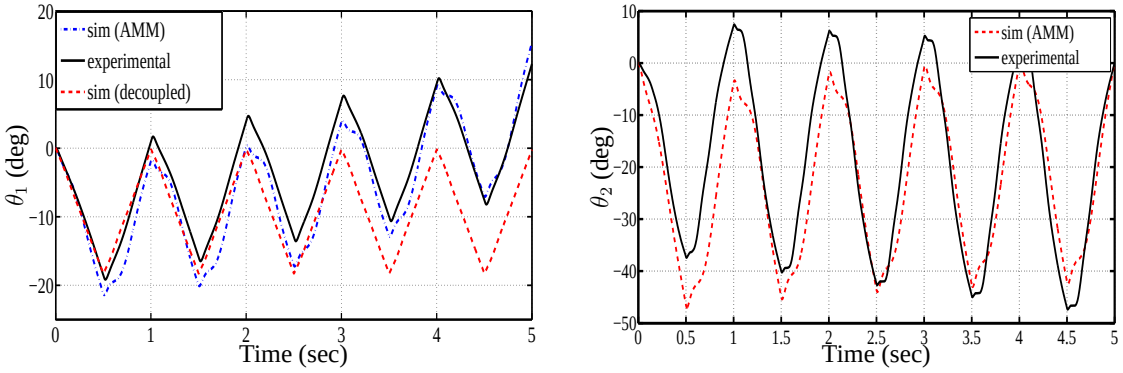

(a) Motor 1 (b) Motor 2

Figure 2.13: Response to square wave input

Figure 2.13 shows the response of motor-1 and motor-2 respectively for square input signal. Figure 2.13(a) compares the response of motor-1 in simulation and in experiment. In simulation, two different models are considered namely the decoupled model and AMM model. It can be seen from Figure 2.13 that AMM model is more closer to actual system than decoupled model. Figure 2.13(b) shows the response of motor-2 to square input signal in simulation and in experiment. It is observed that for same torque amplitude, the deflections of link2 is more than link1 since joint-2 is pinned one.

The following were quantitative results to denote modeling errors.

Strategy	$\|e_{\theta_1}\|$	$\|e_{\theta_2}\|$
AMM	112.88	153.56
Decoupled	289.34	301.2

Table 2.3: Comparison of performance for SMC and FSMC in simulation

- Error between actual plant and decoupled model for actuation angle θ_1 is; $\|e\|_1 = 289.34$
- Error between actual plant and AMM model for actuation angle θ_1 is; $\|e\|_1 = 112.88$

It is clear that AMM model is more closer to the actual plant.

2.7 Summary

The chapter described the systematic development of dynamic model of single link and two link flexible manipulators. The model for SLFM has been developed by assuming the flexible link as a rotary spring. The model for TLFM has been developed by decoupled approach and AMM approach. Experimental set up considered for model development also have been discussed in detail. The mathematical models have been validated using these experimentation.

In case of SLFM, model is linear (due to lumped parametric approach). In case of TLFM, the decoupled approach gives a simple but approximate model and AMM approach generates more accurate model, wherein the flexibility is captured adequately due to distributed parametric approach. Also, the derived mathematical models have been validated by verifying closeness of model output and experimental output when excited by same input. It is confirmed that the dynamic model obtained by AMM is appropriate enough to represent the physical TLFM system. These developed models are used for testing performance of model based control strategies using sliding modes in the subsequent chapters.